International Journal of Physical Sciences Vol. 5(3), pp. 238-245, March 2010
Available online at http://www.academicjournals.org/IJPS
ISSN 1992 - 1950 © 2010 Academic Journals

Full Length Research Paper

Two-dimensional electrical resistivity survey around the periphery of an artificial lake in the precambrian basement complex of northern Nigeria

I. B. Osazuwa[1] and E. Chii Chii[2]*

[1]Department of Physics, Ahmadu Bello University, Zaria, Kaduna State, Nigeria.
[2]Department of Physics, Adamawa State University, Mubi, Adamawa State Nigeria.

Accepted 28 January, 2010

A two-dimensional electrical resistivity survey was carried out at the periphery of the impounding reservoir of the Ahmadu Bello University farm dam in order to investigate the subsurface seepage conditions and identify possible weak zone that could serve as seepage paths within the subsurface in the vicinity of the dam. Eight profiles were acquired, using Abem Lund imaging system, along each of the northern and southern abutment (flanks) of the reservoir. The RES2DINV interpretation software was used to analyze the data and the resulting tomograms, generally, it shows a resistivity variation from 23 to 926 Ωm. Anomalous low resistivity zones within the bedrock are interpreted as zones of weakness representing preferential flow pathways for water from the impounding reservoir.

Key words: Two-dimensional, electrical resistivity, subsurface seepage condition, artificial lake, Nigeria.

INTRODUCTION

The Ahmadu Bello university Farm dam provides tremendous benefits, including water supply for drinking, recreation and irrigating the experimental farms of the faculty of agriculture of the University. Without proper maintenance, however, a dam may become unable to serve its intended purpose and could be at great risk in failure.

Effective dam inspection programs routinely identify deficiencies at dams, but inspections alone are not adequate to identify all the defects especially those occurring at the subsurface where a visual assessment cannot be identified. Such assessments are usually limited to the surface and subsurface assessments can only be carried out with the help of geophysical techniques (Bogoslovsky and Ogilvy, 1970; Butler et al., 1989; Abuzeid, 1994; Sirles, 1997; Aal et al., 2004; Lim et al., 2004; Song et al., 2005).

The A.B.U. farm dam is aging and the reservoir is no longer filled to capacity for a greater portion of the year except at the heart of the rainy season and as observed by Butler et al, 1989, frequently occurring geotechnical problem associated with such an aging infrastructure is the development of anomalous seepage paths.

This work aims at investigating the subsurface conditions around the periphery of the lake to detect weak zones favorable for seepage at the flanks of the dam. Such weak zones are usually products of weathering and\or fracturing of the bedrock which are identifiable as resistivity low in a resistivity tomogram.

Geology of the study area

The impounding reservoir together with its watershed (19,247,000 m^2) is underlain by the biotite gneiss belonging to the precambrian basement complex of northern Nigeria (Figure 1). It is therefore a metamorphic terrain bounded in the west by quartz-mica schist and in the east by biotite granite believed to have intruded the basement gneiss during the Pan African Orogeny according to McCurry (1970). The greater part of the area is covered with thick regolith mainly derived from *in-situ* weathering of the basement rocks. Some areas on the watershed are capped by lateritic material.

METHODOLOGY

The study involved a preliminary survey, followed by electrical

*Corresponding author. E-mail: chiiemma@gmail.com.

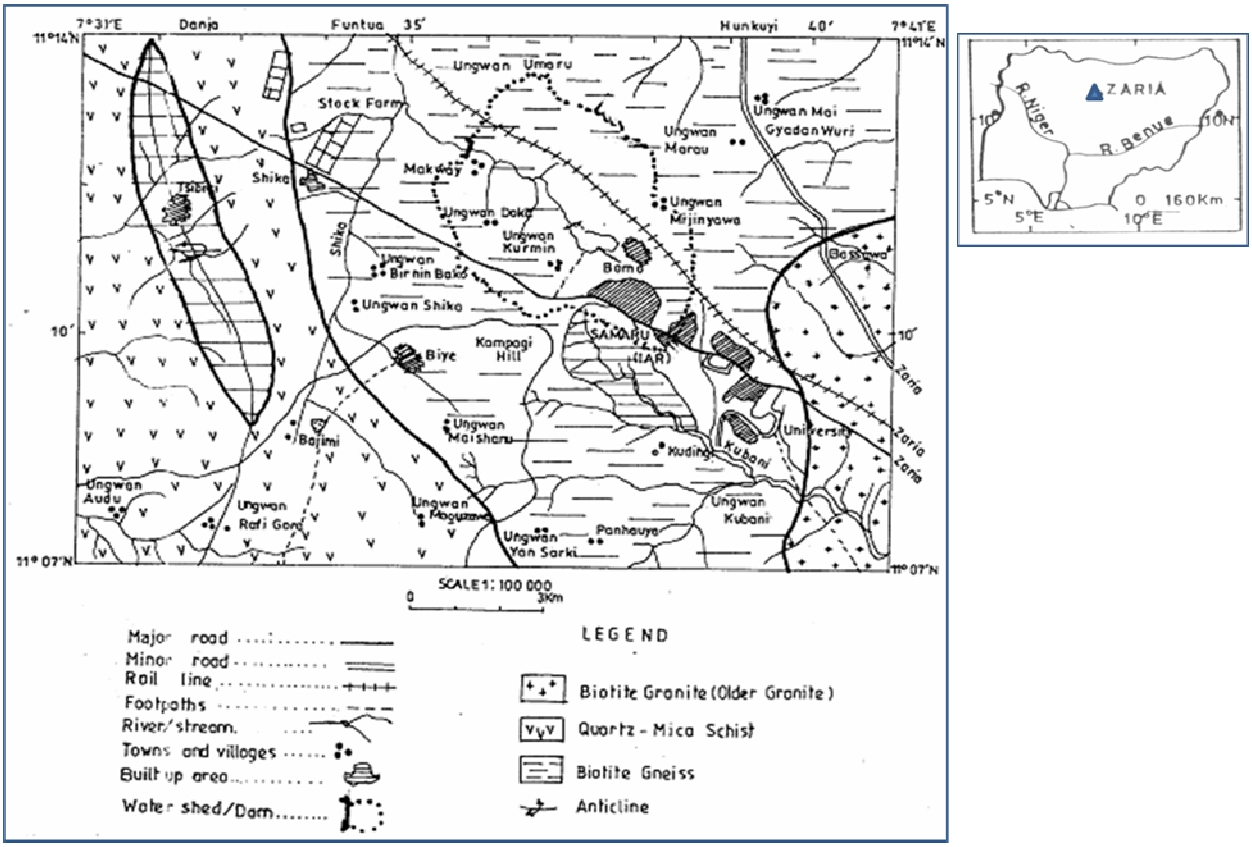

Figure 1. Geological map of the study area (modified from McCurry, 1970).

resistivity measurements and interpretation of measured data by using computer software in the laboratory. The preliminary work involved a number of tasks: Mapping the boundaries of the open water table of the impounding reservoir using satellite navigator; producing a map (Figure 2) showing the configuration of ground-water flow in the area and finally, selecting profile lines for the resistivity data acquisition.

The 2D resistivity method

Resistivity determinations are usually made by injecting a specified amount of electric current into the ground through a pair of current electrodes and then, with the aid of a pair of potential electrodes, measure the potential difference between any two points at the surface caused by the flow of the electric current in the subsurface. From the measured current (I) and the voltage (V) values, the ensuing resistivity is determined.

The ABEM Lund Imaging system comprising of Terrameter SAS 4000 supplemented with an automated multi-electrode system was used in collecting the 2D electrical resistivity data. The Wenner32SX protocol dedicated for Wenner-α CVES roll-along measurement with 2 cables was employed because of its high signal – to – noise ratio, with a unit electrode spacing of 5 m. The profile lines along which the data were collected (P_1 - P_8) and are shown, to scale, in Figure 3. P_1 to P_4 occupy the southern flank and P_5 to P_8 occupy the northern flank of the reservoir. The lengths of profiles range from 300 to 600 m. Results of the survey on the embankment shown in Figure 3 have been reported in Osazuwa and Chii, 2009.

Data analysis

The raw data obtained for this work, comprising of measured apparent resistivity, were processed using the computer program RES2DINV (Geotomo Software, 2001). Interpretation of a 2D set of data requires a 2D model of the subsurface.

The 2D model used by the program divides the subsurface into a number of rectangular blocks. The program then determines the resistivity of the rectangular blocks that produces an apparent resistivity pseudosection (calculated apparent resistitivity) which agrees with the actual measurement. A finite-difference forward modeling subroutine was used to calculate the apparent resistivity values. A relatively dense mesh grid of 4 nodes per unit electrode spacing was used in the forward modeling to increase the accuracy of the calculated apparent resistivity though computationally expensive in terms of time. The thickness of the first layer of blocks was set at 0.5 times the unit electrode spacing; the thickness of each subsequent deeper layer was increased by 10%. A non-linear least-squares optimization technique (deGroot-Hedlin and Constable 1990; Loke and Barker 1996) was used for the inversion routine. All inversion methods essentially try to find model for the subsurface whose response agrees with the measured data. In the cell-based method used by the RES2DINV software, the model parameters are the resistivity values of the model blocks, while the data is the measured apparent resistivity. The optimization method basically tries to reduce the difference between the calculated and measured apparent resistivity values by iteratively adjusting the resistivity of the model blocks. A measure of this difference is given by the root-mean-squared (RMS) error. The model at the iteration after which the RMS error does not change significantly is usually

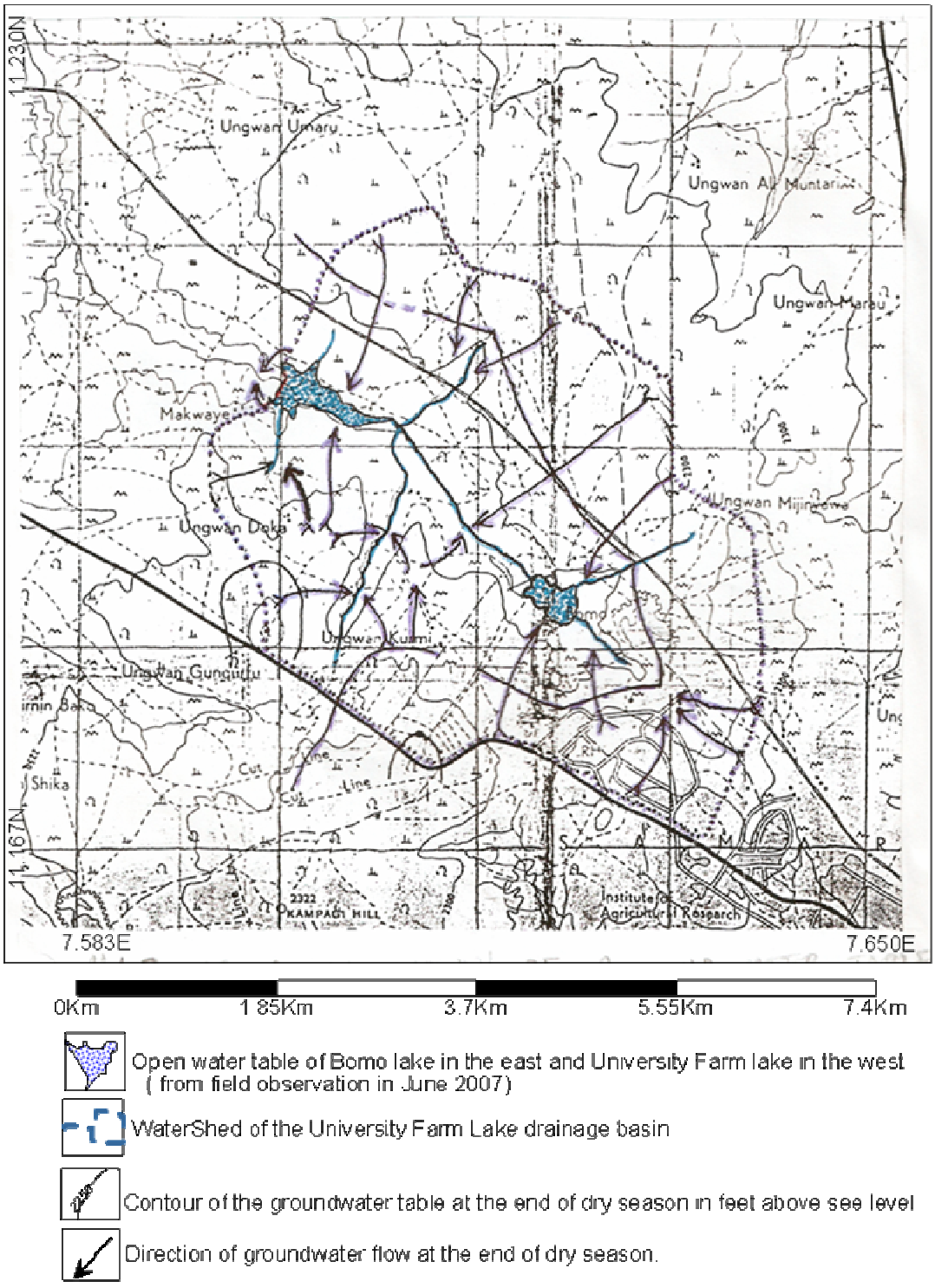

Figure 2. Map of configuration of groundwater table and directions of groundwater flow at the end of the dry season.

considered the “best” model and in this work, this occurred between the 5th and 7th iterations.

One advantage of this method is that the damping factor and the flatness filters can be adjusted to suit different types of data. Since the data obtained in this work are less noisy, an initial damping factor of 0.1 was used and the minimum was tagged at 0.02 (one-fifth of the initial) to stabilize the inversion process. The inversion routine generally reduces the damping factor after each iteration and the smooth models obtained have the ability to suppress model structures not required by the data. The generated models

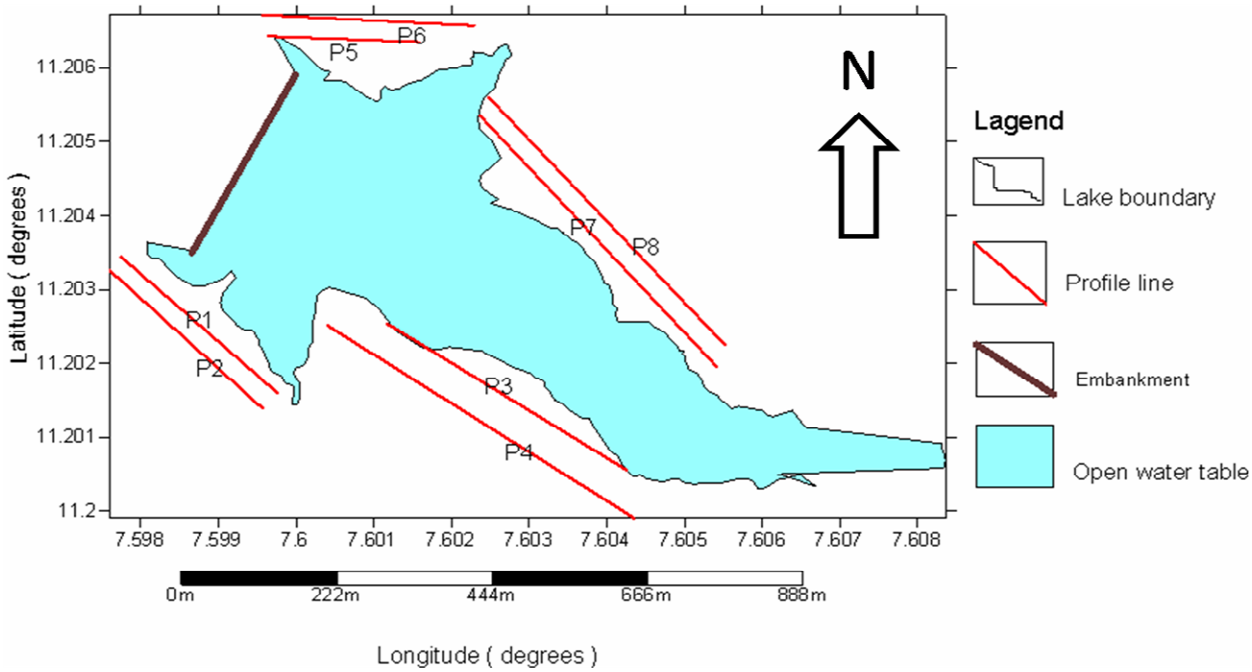

Figure 3. Location of profiles around the lake.

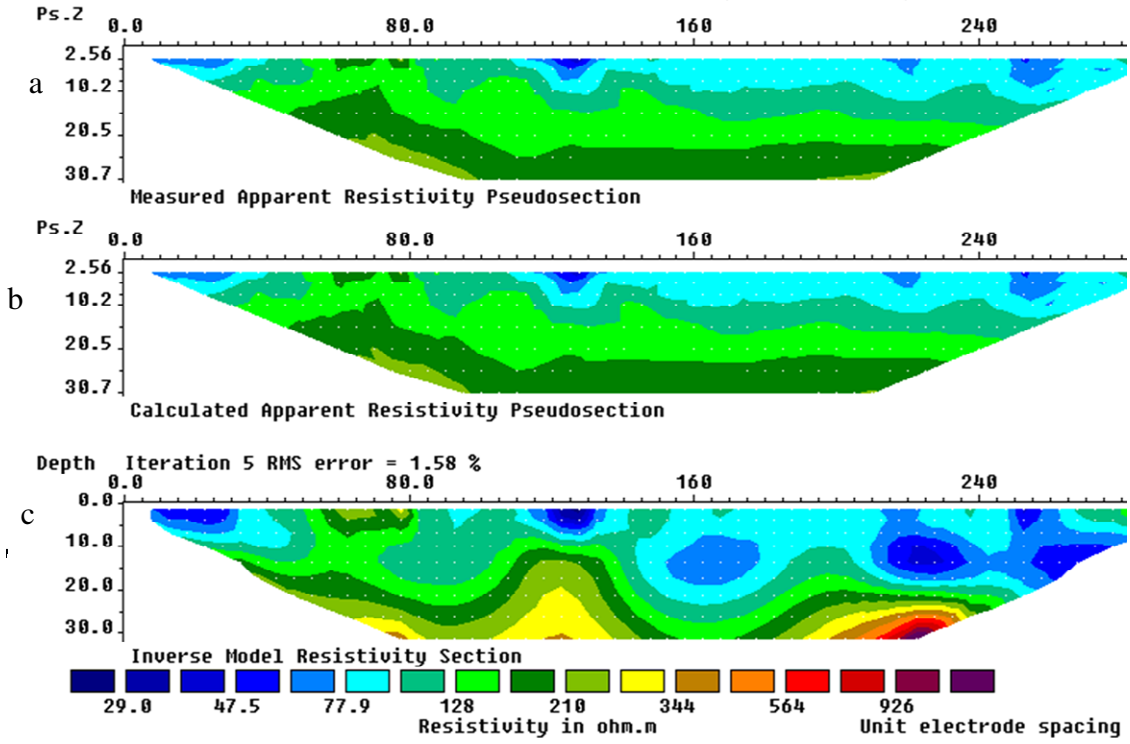

Figure 4. (a) The observed and (b) calculated apparent resistivity pseudosection with (c) the inverse model resistivity section for the data set along traverse P_1.

therefore contain the minimum possible structures and is then likely that the true earth is at least as rough as the models (deGroot-Hedlin and Constable, 1990) thereby increasing the probability that identified anomalies are actually existent.

The 2D model resistivity sections obtained for each of the profiles shown in Figure 3 were used to deduce the possible lithologic sections (Figures 4 - 8) by using information from a borehole log drilled within the study area (Table 1) and geology of the area

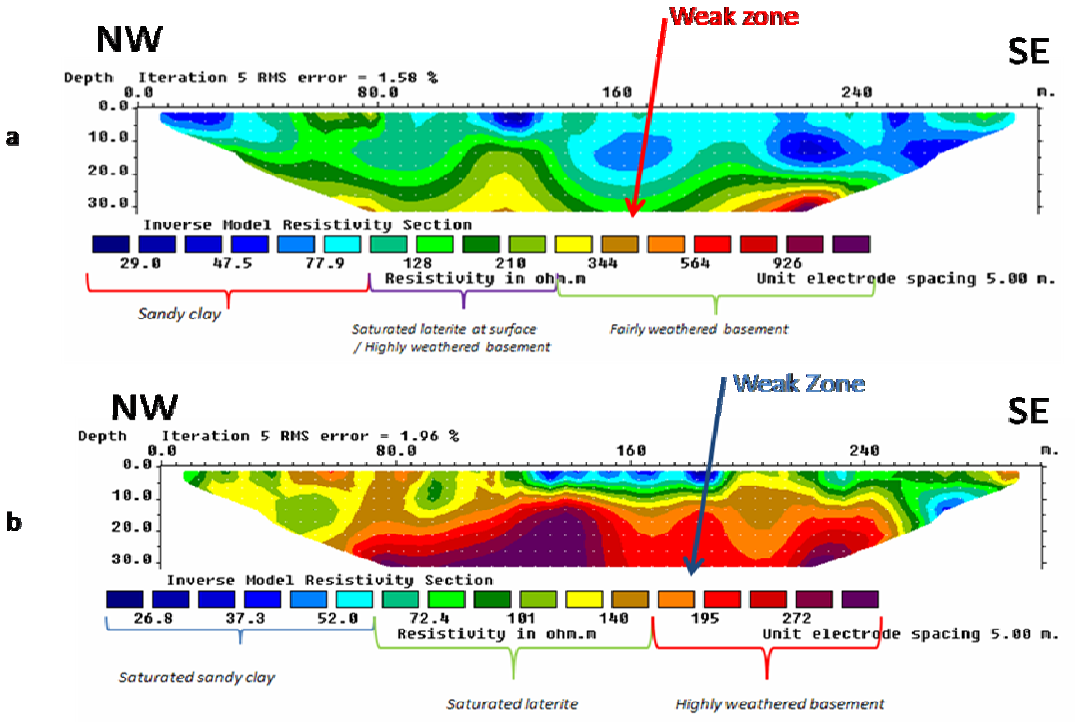

Figure 5. (a) Werner configuration inverted resistivity section along traverse P_1 and (b) P_2 showing assigned lithology and anomally of interest (weak zone within bedrock).

Table 1. Lithology and aquifers borehole log (NWRI, 2002).

Depth (m)		Thickness (m)	Lithology
From	To		
0	15	15	Reddish brown laterite
15	21	6	Brownish sandy clay
21	42	21	Weathered basement
42	-	-	Fresh crystalline rock

according to McCurry (1970).

RESULTS AND DISCUSSION

From the flow directions of water in the dam's drainage basin shown in Figure 2, it can be ascertain that the impounding reservoir is effluent with recharge favored through the flanks than seepage. This excludes the possibility of seepage taking place through loose grounds of the overburden which is usually a target anomaly in other seepage assessment projects. Thus any seepage along the flanks can most probably take place through deep seating weak zones (faults, joints, fractures, intensely weathered zones etc) within the bedrock, all of which are detectable in a resistivity tomogram as resistivity low within a frame work of resistivity high.

The complete set of geoelectrical images (measured apparent resistivity pseudosection, calculated apparent resistivity pseudosection and the inverse model resistivity section) for the first profile P_1 , for example, are shown in Figure 4. About seven geoelectric segments are encountered in this profile with each segment represented by a distinct colour. The reliability of the inverse model resistivity section (Figure 4c) is reflected in the degree of agreement between the measured and calculated apparent resistivity pseudosections (Figures 4a and 4b). This can be easily seen by visual inspection of the two images (Figures 4a and 4b) and also from the low RMS error (1.58% in this case).

Meaningful geological interpretation of the inverse model resistivity section is done using geologic information of the area (McCurry, 1970) and information from borehole log (Table 1). Combining these information with the range of resistivity values encountered in the inverse model resistivity sections for all the profiles investigated in this work (Figures 5 - 8), a lithological unit-base model

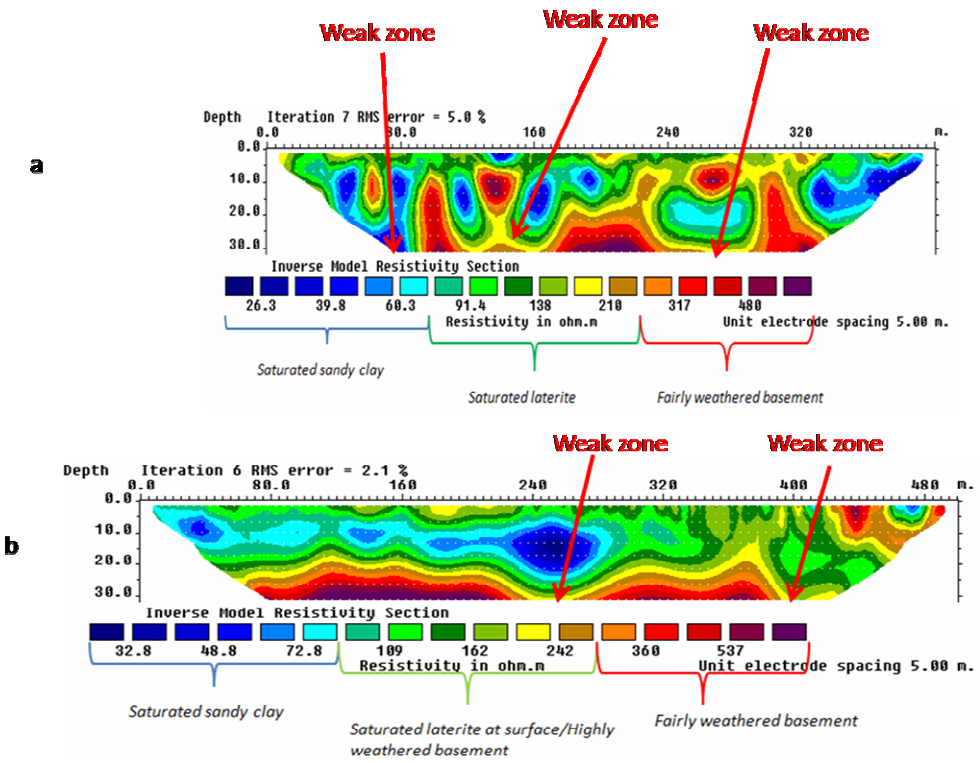

Figure 6. (a) Werner configuration inverted resistivity section along traverse P_3 and (b) P_4 showing assigned lithology and anomaly of interest (weak zone within bedrock).

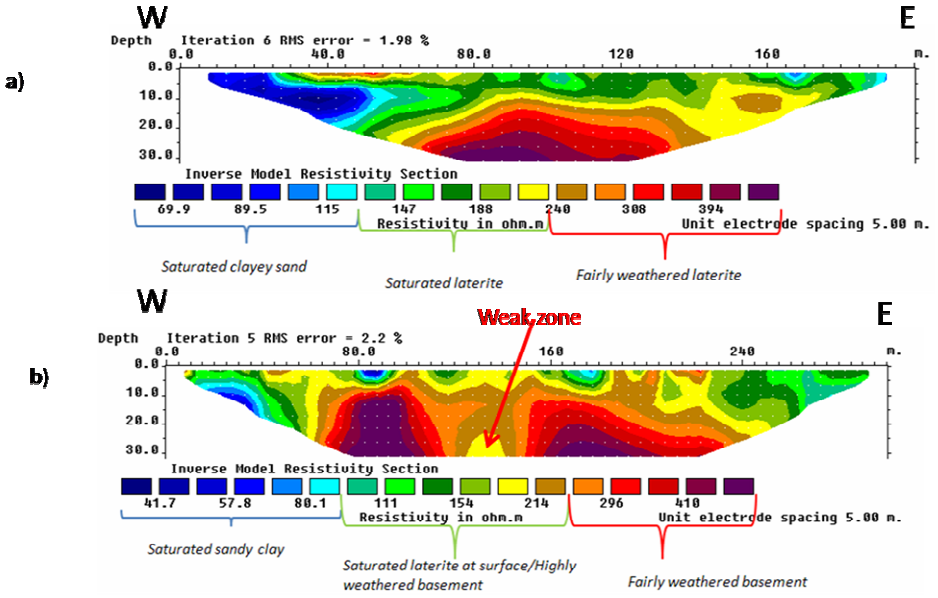

Figure 7. (a) Werner configuration inverted resistivity section along traverse P_5 and (b) P_6 showing assigned lithology and anomaly of interest (weak zone within bedrock).

classification is derived (Table 2) for the interpretation of the inverse model resistivity sections obtained. The seven geoelectric segments in the inverse model resistivity section for the first profile (Figure 4c) constitute three distinct geologic layers based on the classification in Table 2. The top layer is composed of saturated sandy

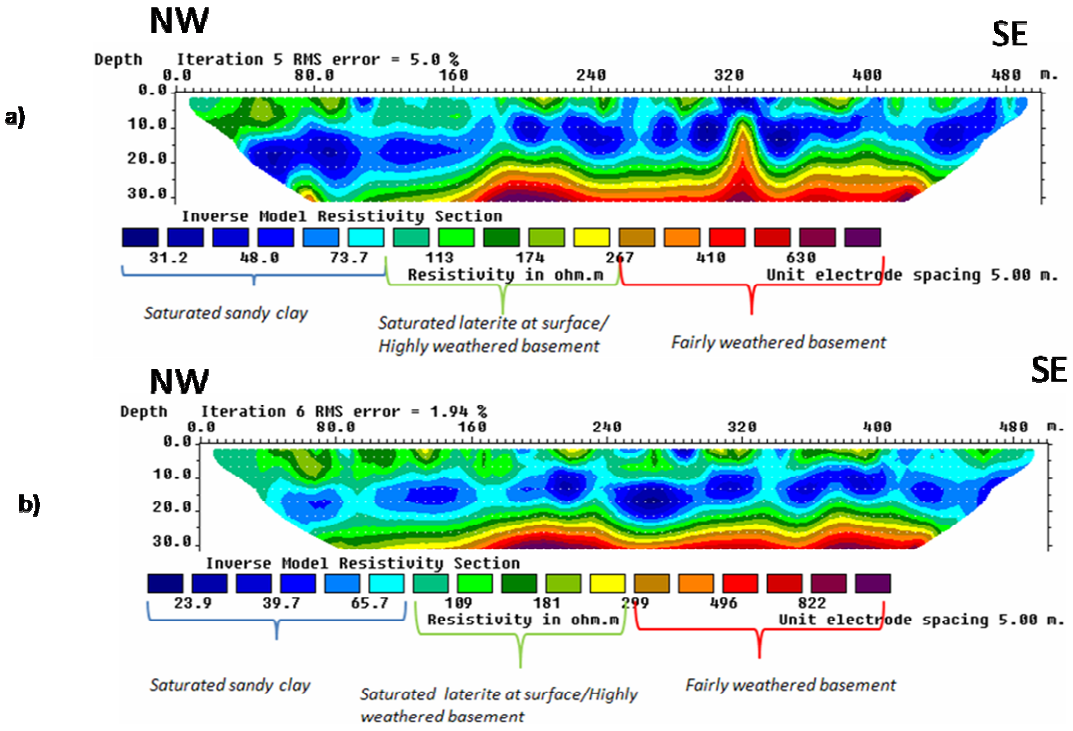

Figure 8. (a) Werner configuration inverted resistivity section along traverse P_7 and (b) P_8 showing assigned lithology and anomaly of interest (weak zone within bedrock).

Table 2. Range of resistivity values and their corresponding geologic interpretation derieved for this work.

Rock types	Resistivity (Ωm)
Saturated sandy clay	24 - 80
Saturated clayey sand	70 - 115
Saturated laterite	72 - 267
Highly weathered basement	109 - 299
Fairly weathered basement	214 - 926

clay (with resistivity range of 29.0 - 80 Ωm) interspersed with saturated laterite (128 - 210 Ωm). This layer varies in thickness from about 10 to 24 m. The second layer with resistivity range of 128 - 210 Ωm is the highly weathered basement having thickness of about 5 to 12 m. The third layer of resistivity range of 344 - 926 Ωm and extending down to the depth of investigation is interpreted to represent the fairly weathered basement. The lateritic potions near the surface, in Figure 4c, have the same resistivity range as the weathered basement beneath. Both layers are therefore distinguished by the depth of occurrence and also by the homogenous nature of the geoelectric segments constituting the weathered basement which is an indication of *in-situ* chemical alteration of the hard rock. The remaining 2D inverse model resistivity sections with their geologic interpretation are shown in Figures 5 - 8 (opposite profiles are placed side-by-side for a visual correlation and identification of anomalies of interest).

Figures 5a and 5b display the inverse model resistivity sections derived for P_1 and P_2 respectively. Both traverse show a surface layer of low to moderate resistivity with P_1 dominated by the low resistivity range of 29 - 80 ohm-m representing saturated sandy clay and a few portions of the moderate resistivity of range 128 - 210 ohm-m interpreted as lateritic top soil which is also saturated. P_2 shows a distribution of similar materials at the surface but with lower range of resistivity values. The 26 - 52 ohm-m range representing saturated clay is sparsely distributed beneath P_2. It occupies the central portion of the profile centered at 160 m along the profile with a length of about 70 m and thickness of about 5 m, while saturated laterite with a range of value of 72 - 140 ohm-m occupies a greater portion of the surface layer. The near surface saturation along these profiles is as a result of irrigation as water is constantly drawn from the dam to water the crops in the nearby farms. The sandy clay and lateritic top layer is underlain by a moderate resistivity layer which ranges from 128 - 210 ohm-m beneath P_1 and 195 - 272 ohm-m beneath P_2 indicating that the basement beneath both profiles is intensely weathered and saturated. These are weak zones which are considered risky where they extend deep into the bedrock as they could provide micro channels for seepage of water from the lake under the effect of hydraulic gradient as the hydraulic pressure increase with depth. It is worth noting

that the fresh basement within this area lies between a depths of 30 to 50 m, so weak zones extending deeper than 30 m are considered to constitute a thread. Beneath this layer in P_1 (Figure 5a) is evidence of harder and fresher rock (yellow color) with resistivity starting from 344 ohm-m and above. However the hard rock does not feature beneath the 160 m mark along the profile rather the highly weathered bedrock extends deeper here and is therefore considered a potential seepage medium. The same argument holds for the weak zones identified in Figures 6 and 7. The first weak zone in Figure 6(a) beneath 80 m mark along the profile starting about 5 m and extending to above 30 m (the depth of investigation) with resistivity of about 40 ohm-m is an indication of intense saturation resulting from water leaking through this weak zone under the influence of changes in the hydraulic gradient with distance from the dam. The hard rock is more prominent in Figure 8, where it occurs at an average depth of about 25 m, except at the western end of the profiles, that is, between 0 - 160 m along the profiles where the depth of weathering and saturation extends beyond the depth of investigation. This portion of the profiles is actually close to one of the streams supplying the reservoir in the northern part, the fact that the fresh bedrock is deeper at this potion is an indication that the stream valley is probably structurally controlled. This is however subject to further investigation.

Conclusion

The images of the subsurface beneath the profiles investigated generally reveal a variation in resistivity from 24 ohm-m to 926 ohm-m with the lowest resistivity value encountered in profile 8 and the highest in profile 1. Three resistivity zones were observed with distinct resistivity values and variable thicknesses. The first resistivity zone (first layer) represents the overburden with variable thickness from 5 to 20 m compose of two resistivity ranges: the first range (24 - 80 ohm-m) represents sandy clay materials while the second range 72 - 267 ohm-m represents lateritic materials. The overburden is therefore composed of an intercalation of lateritic and sandy clay materials rich in moisture content. The second resistivity zone with a resistivity range of 109 - 299 ohm-m and thickness varying from 5 to 10 m is the highly weathered basement. The third resistivity zone represents the fairly weathered bed rock and shows a higher resistivity value ranging from 214 - 926 ohm-m. In some areas, the high resistive layer representing the fresher bedrock has been intensely weathered resulting in portions of moderate resistivity, such an intensely weathered portion of the bedrock suggest a possible seepage conduits for water flow. These portions have been identified in the tomograms and indicated by arrow lines. Active seepage is most probably taking place at the weak zone identified in profile P_3 in Figure 6a beneath the 80 m mark where the bedrock shows an anomalous low resistivity, below 40 ohm-m. Based on the above discussion and conclusion, we are recommending injection grouting at the weak zones identified.

ACKNOWLEDGEMENTS

We wish to acknowledge the International Programme in the Physical Sciences (IPPS), Uppsala University Sweden for providing the equipments and part of the funding of this work. Also, our gratitude to Professor K. Schoeneich of geology department, Ahmadu Bello University, Zaria, Nigeria, for the contributions made in this research work.

REFERENCES

Aal Gamal ZA, Ahmed MI, Neil LA, Estella AA (2004). Geophysical Investigation of Seepage from an Earth Fill Dam, Washington County, Mo. www.dot.state.fl.us.

Abuzeid N (1994). Investigation of channel seepage areas at the existing Kaffrein dam site (Jordan) using electrical-resistivity measurements. J. Appl. Geophys. 32: 163-175.

Bogoslovsky VA, Ogilvy AA (1970). Application of geophysical methods for studying the technical status of earth dams. Geophysical Prospecting 18: 758-773.

Butler KD, LLopis LJ, Deaver MC (1989). Comprehensive geophysical investigation of an existing dam foundation, The leading Edge of exploration, pp.10-18.

DeGroot- Hedlin C, Constable S (1990). Occam's inversion to generate smooth, two- dimensional models form magnetotelluric data. Geophys. 55: 1613- 1624.

Geotomo Software (2001). RES2DINV Ver. 3.4 for Windows 95/98/Me/2000/NT/XP-program for Rapid 2-D Resistivity and IP inversion using the least-squares method (available at www.geoelectrical.com).

Lim HD, Kim KS, Kim JH, Kwon HS, Oh BH (2004). Leakage detection of earth dam using geophysical methods. Procs. International Commission on Large Dams (ICOLD), 72th Annual Meeting, 16-22 May 2004, Seoul, Korea: 212-224.

Loke MH, Barker RD (1996). Rapid least- squares inversion of apparent resistivity pseudosections by a quasi- Newton method. Geophys. Prospect. 44: 131- 152.

McCurry P (1970). The Geology of Degree Sheet 21 Zaria. Unpublished MSc. Theses, A.B.U. Zaria.

NWRI (2002). Borehole completion report at ABUTH Hostel, Groundwater Research Department, National Water Resource Institute, Kaduna, Nigeria.

Osazuwa IB, Chii EC (2009). A two-dimentional electrical resistivity imaging of an earth dam, zaria, nigeria. J. Environ. Hydrol. Vol. 17 paper 28 October 2009, published by the International Association for Environmental Hydrology on the World Wide Web at http://www.hydroweb.com.

Sirles P (1997). Seepage investigation using geophysical technigues at Coursier Lake Dam, B.C., Canada. Symposium of the Geophysical Application to Environmental and Engineering Problems (SAGGEP), Reno-Nevada, 1: 321-331.

Song SH, Song YH, Kwon BD (2005). Application of hydrogeologica and geophysical methods to delineate leakage pathways in an earth fill dam. Exploration Geophysics 36: 92-96.